Optics Letters

triSPIM: light sheet microscopy with isotropic super-resolution

James D. Manton* and Eric J. Rees

Department of Chemical Engineering and Biotechnology, University of Cambridge, Cambridge CB2 3RA, UK
**Corresponding author: ajdm2@cam.ac.uk*

Received 23 June 2016; revised 1 August 2016; accepted 4 August 2016; posted 4 August 2016 (Doc. ID 268634); published 7 September 2016

We propose a three-objective light sheet microscopy geometry which, through a combination of skewed lattice light sheet excitation through two objectives and the computational fusion of images taken from two separate lens pairings, would allow for isotropic super-resolution in mesoscopic samples. We also show that simultaneous coherent excitation through two excitation objectives could further substantially increase resolution. Simulations demonstrate that our design could achieve a resolution of 120 nm for EGFP imaging while minimizing photodamage.

OCIS codes: (180.6900) Three-dimensional microscopy; (100.6640) Superresolution; (180.2520) Fluorescence microscopy; (050.1940) Diffraction.

http://dx.doi.org/10.1364/OL.41.004170

Light sheet microscopy (LSM) is a powerful tool for cell and developmental biology and allows for the acquisition of large volumetric datasets at high speed [1]. In contrast to confocal microscopy, in which most of the sample is illuminated at once and a pinhole is used to reject out-of-focus light in a raster scanning approach, LSM uses orthogonal illumination and detection pathways in which a sheet of light is used to illuminate a thin section of the sample at a time, with the resulting fluorescence being detected on a camera [see Fig. 1(a)]. This simultaneously increases the imaging speed and reduces phototoxicity, but at the cost of reduced resolution due to the requirement to use lower numerical aperture lenses that are compatible with the orthogonal geometry required. In addition, the "side-on" illumination used results in shadowing in the propagation direction when an object occludes the light sheet.

There has been considerable recent interest in increasing both the lateral and axial resolution of LSM with a number of methods having been developed, including altering the beam profile of a "virtual" light sheet (in which a pencil-like beam is rapidly scanned across the sample in one camera exposure) from a standard Gaussian beam to a Bessel or Airy beam [2,3]; using structured illumination microscopy (SIM) techniques with a patterned light sheet to computationally reconstruct super-resolved images [4] and combining LSM with stimulated emission depletion to effectively reduce the width of the beam below the diffraction limit [5]. Alternatively, by using each of the perpendicular objectives for both illumination and detection, and computationally fusing the resulting datasets, an isotropic resolution is achieved using normal Gaussian light sheets [6]. Shadowing has previously been reduced by tilting the light sheet in-plane during an exposure and by using two opposed excitation objectives [7]. Each method has its own advantages and disadvantages, but no method provides isotropic super-resolution.

We propose a three-objective LSM system to provide isotropic super-resolution in which all objectives are identical and positioned at the corner of a cube, which we term triSPIM [see Fig. 1(b)]. By using appropriately sized objectives (such as the Nikon MRD07420), this can be achieved while allowing the use of an iSPIM geometry [8], such that samples can be conventionally mounted on a 5 mm diameter circular cover slip with the objectives being suspended above [see Fig. 1(c)]. By developing skewed versions of the lattice light sheets first described by Chen *et al.* [9], we obtain an isotropic in-plane resolution enhancement through SIM principles while minimizing out-of-plane fluorescence and phototoxicity. We term this maximally orthogonal detection-excitation nanoscopy in thin sheets (MORDENTS) and show it can achieve an in-plane resolution of ~235 nm for EGFP imaging. In addition, by using coherent excitation through two objectives simultaneously, we produce lattice light sheets featuring even finer patterning, allowing SIM reconstructions with improved lateral resolution, in a method we term twinned-MORDENTS requiring interfering lattice light sheets (TRILLS). In combination with the multi-view computation fusion technique of diSPIM [6], this allows such a system to image in 3D at high speed with an isotropic lateral resolution of ~120 nm and an axial resolution of ~190 nm.

Lattice light sheets were simulated using Debye vectorial diffraction theory, calculated using the Fourier transform method of Leutenegger *et al.* described in [10], for a 0.8 NA water-immersion lens at 488 nm, as provided in Code File 1 [11]. An isotropic voxel size of 66.7 nm was used so that excitation profiles from two orthogonal objectives could be directly superposed, satisfying the Nyquist sampling criterion over a 40 μm field-of-view without requiring excessive computer memory.

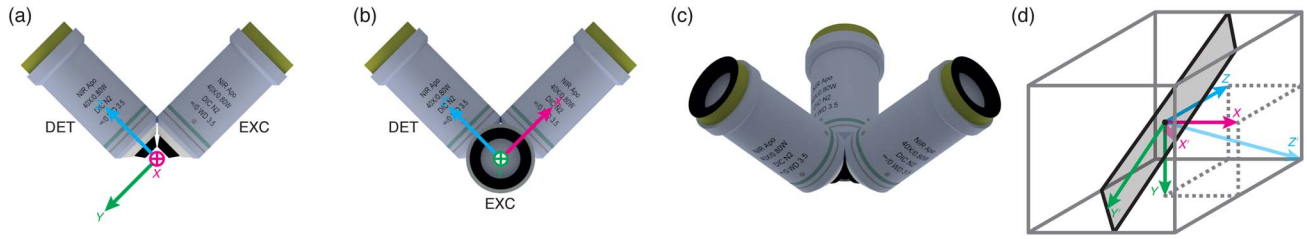

Fig. 1. (a) Conventional SPIM geometry with two matched objectives. (b) triSPIM geometry with three objectives, looking down one objective. In (a) and (b), X is the fast scanning axis, Y is the beam propagation direction, and Z is the slow scanning axis, with EXC as the excitation objective and DET as the detection objective. (c) Rotated view of (b) showing inverted SPIM compatibility. (d) Coordinate systems for triSPIM geometry with axes as in (b). Cutting plane, i.e., the effective lateral plane of TRILLS, is (111) with $X' = [10\bar{1}]$, $Y' = [\bar{1}2\bar{1}]$, and $Z' = [111]$.

While using higher NA objectives would immediately result in higher resolution, objectives with numerical apertures greater than 0.8 but that would still physically fit together so that their focal points are coincident, are not commercially available.

Figure 2(a) shows the back aperture illumination required to produce a SIM-compatible, hexagonal lattice light sheet illumination pattern, shown from the excitation objective point of view in Fig. 2(b) and the detection objective point of view in Fig. 2(c). This recapitulates the in-plane results of Chen *et al.* shown in [9], and demonstrates the light sheet's axial propagation. While this allows for maximal resolution enhancement in one direction, no resolution enhancement in the perpendicular direction is possible. Patterning in the propagation direction is possible, but due to the nature of the optical transfer function as spherical caps of the Ewald sphere, only a low patterning frequency can be realized. Indeed, for a 0.8 NA lens, the maximum theoretical axial patterning frequency is six times lower than that achievable laterally, producing an almost negligible super-resolution enhancement of around 15%.

For isotropic SIM resolution enhancement, three patterns oriented at 60 deg to one another are required [12]. Again, due to the fundamental limitations of the optical transfer function, a pattern of fringes oriented at 60 deg to the optical axis would necessarily have a low frequency. However, a pattern at 30 deg could have a much higher fringe frequency, and could be transformed into a pattern at the 60 deg required if it were produced using a second objective oriented at 90 deg to the first. Figure 2(d) shows the back aperture illumination required to produce a light sheet skewed to 30 deg, shown from the excitation and detection views in Figs. 2(e) and 2(f), as before. Using this, an isotropic lateral resolution enhancement of ~25% is achieved. In combination with a moderate Stokes' shift, this effectively gives the 0.8 NA detection objective the resolving power of a 1.1 NA lens, which would not normally fit into a LSM geometry, albeit one that requires multiple raw images to be acquired to produce the same resolution.

Rather than sequentially illuminating with each excitation objective to produce the necessary fringe patterns, simultaneous illumination with coherent light could be used to produce higher frequency fringe patterns through interference [13]. Figure 3(a) shows the modulation transfer function (MTF)

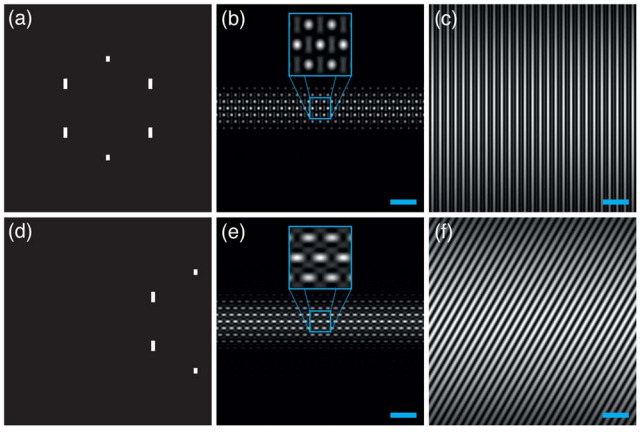

Fig. 2. Simulation of MORDENTS excitation using the Debye diffraction theory, with cyan scale bars corresponding to 5 μm. Cyan insets in (b) and (e) are 3× zoom. Back aperture stripes in (a) and (d) have been horizontally enlarged 11-fold for clarity. (a) Back aperture illumination for an unskewed SIM lattice light sheet. (b) Excitation objective focal plane illumination intensity for (a). (c) Detection objective focal plane illumination intensity for (a). (d) Back aperture illumination for a skewed SIM lattice light sheet. (e) Excitation objective focal plane illumination intensity for (d). (f) Detection objective focal plane illumination intensity for (d).

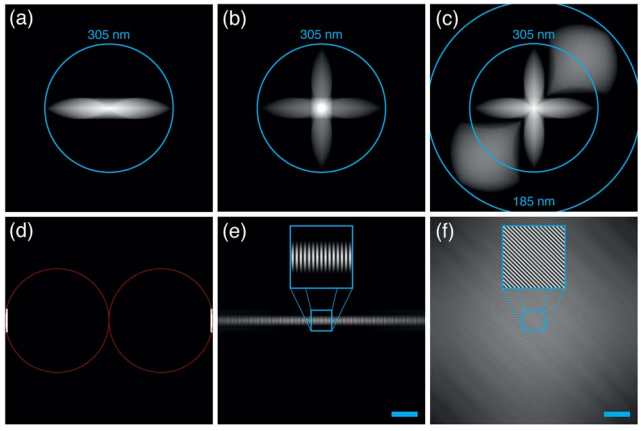

Fig. 3. Simulated illumination MTFs (log-scaled sum projections) and patterns. Cyan scale bars correspond to 5 μm, with cyan insets being 3× zoom. (a) 0.8 NA excitation MTF viewed along the detection axis. (b) Dual 0.8 NA excitation MTFs for incoherent or sequential illumination along both excitation axes, viewed along a detection axis. (c) Dual coherent a 0.8 NA excitation MTF, viewed along a detection axis. (d) Back aperture illumination for TRILLS light sheet. Each circle (red in color online) corresponds to one objective. Pattern stripes have been horizontally enlarged 11-fold for clarity. (e) Illumination intensity for (d) viewed in the plane of one excitation objective. (f) Detection objective focal plane illumination intensity for (d).

for a single lens, with Fig. 3(b) showing the MTF for two lenses oriented perpendicular to one another and used sequentially, as in MORDENTS. Figure 3(c) shows the MTF for coherent illumination through both objectives simultaneously and clearly demonstrates that a much higher frequency can be generated. Figure 3(d) shows the back aperture illumination required to produce a high-frequency lattice light sheet, shown from one excitation objective in Fig. 3(e) and from a detection objective in Fig. 3(f). We propose that such a TRILLS system, operating in a "fusion mode" and using the computational image fusion technique of diSPIM described in [6], would provide a resolution in advance of any current LSM method, attaining a lateral resolution of 120 nm and an axial resolution of 190 nm for EGFP imaging. Figure 4 compares the MTFs of conventional SPIM, MORDENTS, and TRILLS and clearly demonstrates the much larger frequency support of TRILLS, while also showing isotropic lateral resolution enhancement.

Table 1 compares a number of different LSM methods, with particular emphasis on their resolution. It is clear that both MORDENTS and TRILLS compare favorably with current super-resolution LSM alternatives in terms of resolution, particularly in the fusion mode, albeit at the expense of slowed acquisition speed due to the need to acquire multiple raw images per reconstructed images. However, with recent advances in reducing the number of raw images required for a SIM reconstruction down from 9 to 4, with minimal reduction in image quality [15], it seems plausible that similar techniques could be applied to MORDENTS and TRILLS. For MORDENTS, this would result in an acquisition time of only 133% of that of a SIM lattice light sheet, while providing isotropic lateral super-resolution, rather than super-resolution in only one direction.

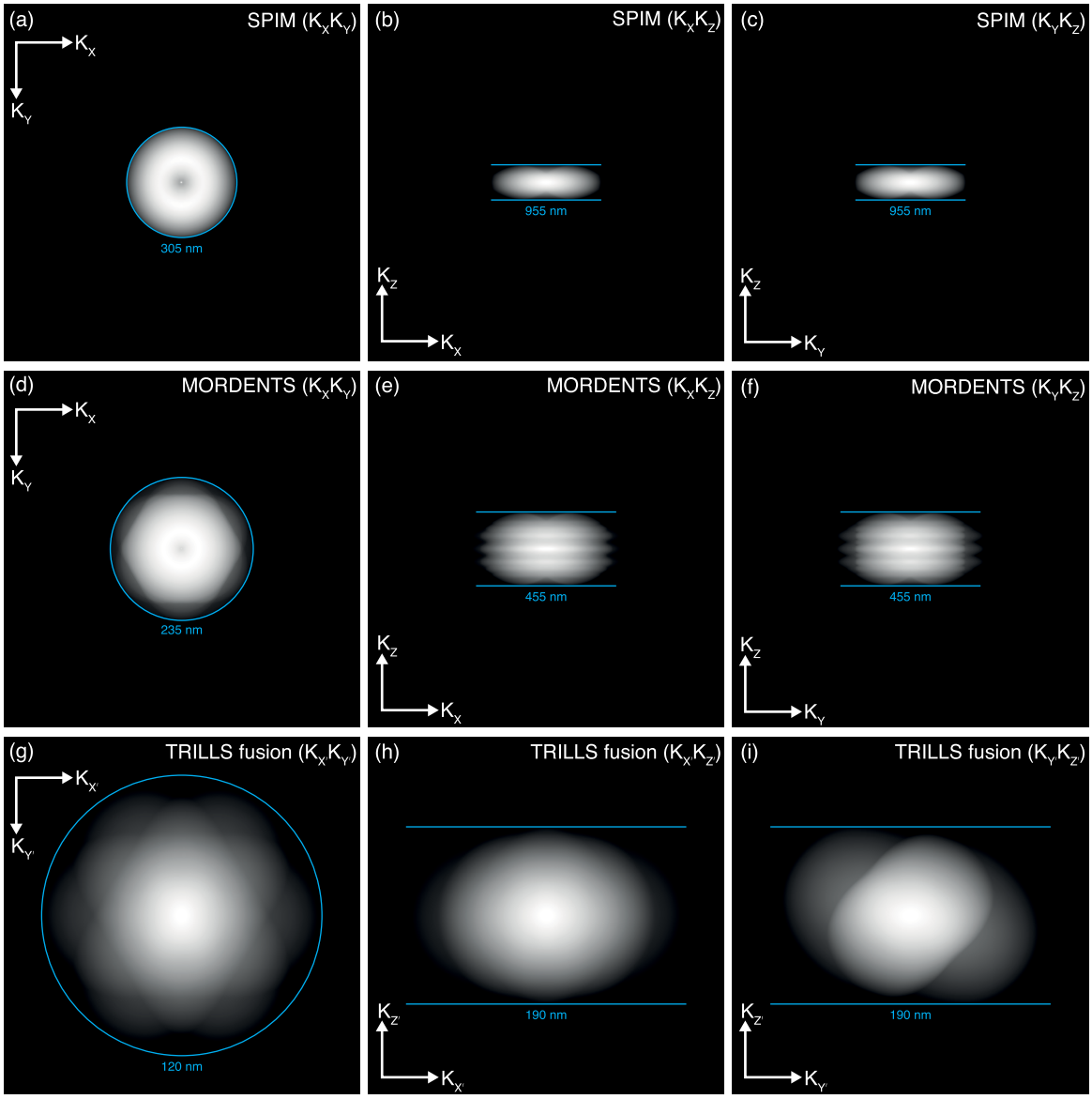

Fig. 4. Overall MTFs (log-scaled sum projections). (a–c) Conventional SPIM MTF, using Gaussian beam illumination, in XY, XZ, and YZ. (d–f) MORDENTS MTF in XY, XZ, and YZ, without image fusion. (g–i) TRILLS fusion MTF in $X'Y'$, $X'Z'$, and $Y'Z'$, where views are fused to computationally produce an enlarged MTF. Note that due to the three-fold mirror symmetry, the MTF appears symmetric in h, but not in I, as these views are 90 deg apart around the $K_{Z'}$ axis.

Table 1. Self-Reported Axial and Lateral Resolutions for Different LSM Methods[a]

Method	Lateral Resolution (nm)	Axial Resolution (nm)	Average Resolution (nm)	Comments	Reference
diSPIM	330	330	330	Requires two raw images per reconstructed image; requires deconvolution for a maximum resolution.	[6]
MORDENTS (Single Mode)	235	455	330	Requires multiple raw images per reconstructed image.	—
Lattice Light Sheet (Dithered)	230	370	285	Requires a custom-made 1.1 NA objective.	[9]
LS-RESOLFT	330	100	275	Special reversibly switchable fluorescent proteins must be used; only an axial resolution enhancement.	[14]
MORDENTS (Fusion Mode)	235	235	235	Requires multiple raw images per reconstructed image.	—
Lattice Light Sheet (SIM)	150/230	280	225	SIM resolution only in one lateral direction; requires a custom-made 0.65 NA objective; requires at least three raw images per reconstructed image.	[9]
TRILLS (Single Mode)	120	265	180	Requires multiple raw images per reconstructed image; increased sensitivity to optical alignment.	—
TRILLS (Fusion Mode)	120	190	145	Requires multiple raw images per reconstructed image; increased sensitivity to optical alignment.	—

[a]"Average resolution" is defined as the square root of the sum of the squares of the resolutions in each dimension, divided by the square root of the number of dimensions.

We note that alternative resolution improvements could be made by using two detection objectives for coherent detection as in I^2M microscopy [16,17]. Alternatively, using three excitation objectives oriented at 120 deg to one another would produce interfering lattice light sheets of maximal fringe frequency. However, this would significantly complicate the optical alignment procedure and would increase the complexity of sample mounting. Adopting the tetrahedral geometry of multiple imaging axis microscopy (MIAM) would allow higher numerical aperture lenses to be used, but would preclude the simple use of interfering lattices [18]. In addition, the difficulties in mounting associated with MIAM were the very problem that led to the development of LSM. MORDENTS, and TRILLS sit between these methods and conventional LSM techniques, with the increased optical complexity being offset by the isotropic super-resolution and the ease of sample mounting provided by the inverted LSM geometry.

Funding. Engineering and Physical Sciences Research Council (EPSRC) Sensor CDT (EP/L015889/1); MedImmune.

Acknowledgment. The authors thank Florian Ströhl and Craig Russell for helpful discussions.

REFERENCES

1. J. Huisken, J. Swoger, F. D. Bene, J. Wittbrodt, and E. H. K. Stelzer, Science **305**, 1007 (2004).
2. T. A. Planchon, L. Gao, D. E. Milkie, M. W. Davidson, J. A. Galbraith, C. G. Galbraith, and E. Betzig, Nat. Methods **8**, 417 (2011).
3. T. Vettenburg, H. I. C. Dalgarno, J. Nylk, C. Coll-Lladó, D. E. K. Ferrier, T. Čižmár, F. J. Gunn-Moore, and K. Dholakia, Nat. Methods **11**, 541 (2014).
4. P. J. Keller, A. D. Schmidt, A. Santella, K. Khairy, Z. Bao, J. Wittbrodt, and E. H. K. Stelzer, Nat. Methods **7**, 637 (2010).
5. M. Friedrich, Q. Gan, V. Ermolayev, and G. S. Harms, Biophys. J. **100**, L43 (2011).
6. Y. Wu, P. Wawrzusin, J. Senseney, R. S. Fischer, R. Christensen, A. Santella, A. G. York, P. W. Winter, C. M. Waterman, Z. Bao, D. A. Colón-Ramos, M. McAuliffe, and H. Shroff, Nat. Biotechnol. **31**, 1032 (2013).
7. J. Huisken and D. Y. R. Stainier, Opt. Lett. **32**, 2608 (2007).
8. Y. Wu, A. Ghitani, R. Christensen, A. Santella, Z. Du, G. Rondeau, Z. Bao, D. Colón-Ramos, and H. Shroff, Proc. Natl. Acad. Sci. USA **108**, 17708 (2011).
9. B.-C. Chen, W. R. Legant, K. Wang, L. Shao, D. E. Milkie, M. W. Davidson, C. Janetopoulos, X. S. Wu, J. A. Hammer, Z. Liu, B. P. English, Y. Mimori-Kiyosue, D. P. Romero, A. T. Ritter, J. Lippincott-Schwartz, L. Fritz-Laylin, R. D. Mullins, D. M. Mitchell, J. N. Bembenek, A.-C. Reymann, R. Böhme, S. W. Grill, J. T. Wang, G. Seydoux, U. S. Tulu, D. P. Kiehart, and E. Betzig, Science **346**, 1257998 (2014).
10. M. Leutenegger, R. Rao, R. A. Leitgeb, and T. Lasser, Opt. Express **14**, 11277 (2006).
11. J. D. Manton, "MATLAB simulation code," University of Cambridge, 2016, http://dx.doi.org/10.17863/CAM.301.
12. M. G. L. Gustafsson, J. Microsc. **198**, 82 (2000).
13. T. Huelsnitz and P. Kner, J. Opt. Soc. Am. A **33**, 179 (2016).
14. P. Hoyer, G. de Medeiros, B. Balázs, N. Norlin, C. Besir, J. Hanne, H.-G. Kräusslich, J. Engelhardt, S. J. Sahl, S. W. Hell, and L. Hufnagel, Proc. Natl. Acad. Sci. USA **113**, 3442 (2016).
15. F. Ströhl and C. F. Kaminski, "Tripling speed in structured illumination microscopy" (in preparation).
16. M. G. L. Gustafsson, D. A. Agard, and J. W. Sedat, Proc. SPIE **2412**, 147 (1995).
17. M. G. Gustafsson, D. A. Agard, and J. W. Sedat, J. Microsc. **195**, 10 (1999).
18. J. Swoger, J. Huisken, and E. H. K. Stelzer, Opt. Lett. **28**, 1654 (2003).